

Structure and Dynamics of Cu₃Au(001) Studied by Elastic and Inelastic Helium Atom Scattering

B. Gans^a, S. K. King, P. A. Knipp^b, D. D. Koleske, and S. J. Sibener

Department of Chemistry and The James Franck Institute, The University of Chicago, Chicago, IL 60637

^aPresent address, Naval Research Laboratory, Code 6177, Washington D. C. 20375

^bDepartment of Physics and The James Franck Institute, The University of Chicago, Chicago, IL 60637

Abstract

We have recently measured the surface phonon spectrum of the ordered binary alloy Cu₃Au(001). In addition to the Rayleigh wave, we observe a higher energy mode which may be interpreted as the "folded" Rayleigh mode or "optical" surface mode. Using a harmonic pair potentials fit to the inelastic neutron scattering data of Katano *et al.*,¹³ we find that the force constant between the first and second layer Cu atoms must be stiffened by 20% with respect to the bulk value in order to match the "folded" Rayleigh mode.

Most experimental and theoretical surface phonon investigations to date have focussed on semiconductor, insulator or pure metal surfaces.¹ Few experimental phonon studies have been undertaken on the surfaces of intermetallic compounds (ordering binary alloys) with the exception of two recent EELS studies on bcc NiAl (111),² (110),^{2,3} and (100).² Intermetallic compounds are of interest due to their high strength characteristics at elevated temperatures.⁴ These remarkable alloys also exhibit increased hardness as compared to either their disordered phase or their single metal constituents.

In this study we examine the Cu₃Au(001) surface, which terminates with a 50% Cu- 50% Au atomic composition in a c(2x2) surface arrangement.⁵ In this orientation the material consists of alternating layers of 50% Cu-50% Au and 100% Cu. This A₃B intermetallic compound, like Ni₃Al, has the minority species occupying the corners of a face-centered cube with (L₁)₂ symmetry. Cu₃Au is

a good model system for investigating how interatomic forces differ between the bulk and surface regions of an intermetallic compound.⁵

Cu₃Au is particularly interesting because the bulk undergoes a first order phase transition ($T_c=663$ K) to form a substitutionally disordered phase at a temperature well below its melting temperature (1226 K).⁵ Recent theories⁶ and experiments⁷ of surface order-disorder transitions indicate that they may occur continuously, but may have some first order character prior to the bulk transition.⁵ Although the symmetry of the lattice is reduced when going from the ordered state to the disordered state, the material retains an fcc lattice--in contrast to a surface melting transition.⁸ This behavior permits investigation of the surface vibrational properties both above and below the transition temperature. We report here the room temperature surface phonon dispersion relations of the ordered state of Cu₃Au(001) along the $\langle 100 \rangle$ azimuth.⁹ Helium atom scattering is well suited for this project as it has excellent sensitivity to the periodic arrangement of the surface, offering superb "contrast" between the topmost and underlying layers. It also serves as both a structural probe, via elastic scattering, and a dynamical one, via inelastic scattering.

The high resolution helium scattering apparatus will be described in a future paper.¹⁰ A short description of it now follows. The machine consists of a helium nozzle beam source, an ultra high vacuum scattering chamber and a rotatable time-of-flight mass spectrometer. The nozzle source can produce a $\Delta v/v$ velocity spread in the incident helium beam of 1%. It is mounted on a closed cycle helium refrigerator, allowing the helium beam energy to be tuned from 8-63 meV. The defining apertures set the beam angular spread to 0.3°. The scattering chamber contains standard UHV preparation (Ar⁺ sputtering gun) and surface analysis tools (AES, XPS, and LEED). The detector consists of a rotatable quadrupole mass spectrometer mounted on optical rails, permitting the crystal-ionizer flight length to be adjusted to either 55 or 100 cm. The detector can independently rotate in the plane of scattering a total of 40 degrees, allowing scattering data to be collected with fixed incident kinematic conditions. An optical encoder mounted on the rotating detector and interfaced to the computer keeps track of the detector angle to 0.01°.

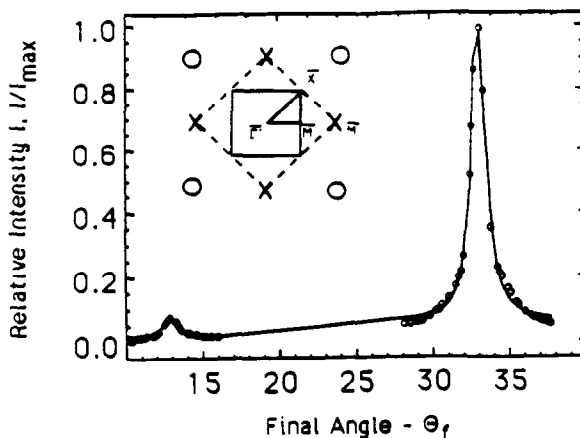


Figure 1: A diffraction scan along the $\langle 100 \rangle$ direction. The solid line is a fit to the data.

The $\text{Cu}_3\text{Au}(001)$ sample, previously used by Graham,¹¹ was placed in UHV without further polishing. The surface was cleaned by cycles of 500 V Ar^+ bombardment and annealing up to 660 K. The crystal was determined to be clean and compositionally ordered when the 60 eV Cu and the 70 eV Au Auger peaks¹² gave a $\text{Cu}_{60}/(\text{Cu}_{60}+\text{Au}_{70})$ ratio of 0.52. After the crystal was cleaned, it was annealed overnight at approximately 630 K in order to enhance the growth of large domains.⁷ The temperature was lowered to 470 K, 1-2 hours prior to scattering. Surfaces prepared in this manner gave sharp full and superlattice LEED diffraction and helium diffraction spots, indicative of the $c(2 \times 2)$ surface arrangement. A diffraction scan along the $\langle 100 \rangle$ direction, showing both the specular and superlattice peaks (open circles), is plotted in Figure 1, along with a fit to the data (solid line) which incorporates the instrument function of the machine. Upon heating the crystal to 663 K, the superlattice diffraction spots disappear, while the full order diffraction spots were still observed. Occasionally the LEED and helium diffraction spots revealed splitting of both the full and superlattice peaks aligned along the $\langle 100 \rangle$ direction, as previously reported by Mc Rae and Malic.⁵

After the crystal was aligned along the $\langle 100 \rangle$ direction using the superlattice diffraction feature, a series of time-of-flight (TOF) measurements were taken using various incident energies ranging from 16-32 meV with the ionizer positioned 55 cm away from the

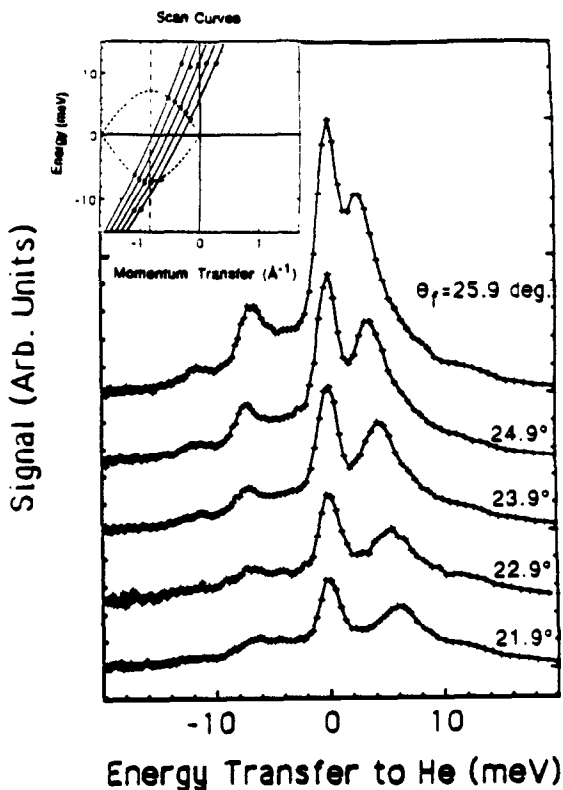


Figure 2: Energy Transformed TOF spectra taken with an incident energy of 31.8 meV and an incident scattering angle of 28.4°. The inset shows the scan curves for the five runs.

crystal surface. In Figure 2 are plotted several energy transformed TOF measurements using a 31.8 meV ($k_i=7.78 \text{ \AA}^{-1}$) helium atom beam, with an incident scattering angle of 28.4° and final angles ranging from 21.9° to 25.9°. Also shown, in the inset of Figure 2, are the scan curves showing the possible energy and momentum transfers for a given detector position. In all TOF spectra, the Rayleigh wave is clearly discernible, along with an intense diffuse elastic signal. In some of the spectra a nearly dispersionless higher energy mode is also observed, essentially a "folded" Rayleigh wave, present because of the smaller surface Brillouin zone (SBZ) of the ordered $c(2 \times 2)$ surface. All of the spectral features plotted in Figure 3 are

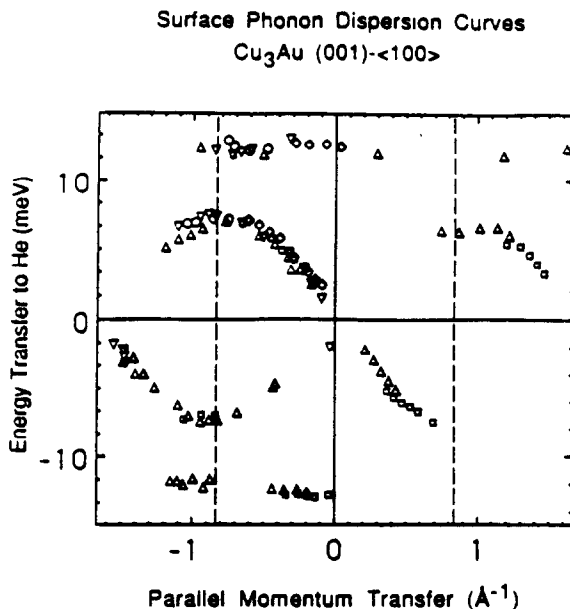


Figure 3: Dispersion curves for Cu₃Au(001) along $\overline{\Gamma} - \overline{M}'$ in the extended zone scheme. Data points with different symbols were taken on different days and correspond to different crystal preparations. Different incident energies and angles were used, and the crystal was approximately room temperature.

displayed in the extended zone scheme along the $\overline{\Gamma} - \overline{M}'$ direction. A total of about 50 TOF runs were taken. All of the collected points are shown in a folded zone scheme in Figure 4. These plots also show two model calculations which will be described below.

To analyze our data we began by modeling the bulk phonon data. A pair potential model [similar to the one used to model the surface modes on NiAl(110)²] was used to fit the bulk phonon data of Katano *et al.*¹³ This model is more restrictive than a Born-von Kármán analysis, and ignores noncentral interactions. The two-body potentials consist of a quadratic part [$= \phi_j'' \times (|r| - |r_0|)^2$], which is essentially the force constant, and a linear part [$= \phi_j' \times (|r| - |r_0|)$], which is a tension between the atoms. Using this model, a nonlinear fit to the bulk phonon data for Cu₃Au was performed, incorporating second nearest neighbor interactions. The results of this seven parameter fit are shown in Table 1.

Table 1.

| j | Atom1-Atom2 | 1st or 2nd neighbor | Bulk Fit in (N/m) | | Surface Fit in (N/m) | |
|---|-------------|---------------------|-------------------|----------------|----------------------|----------------|
| | | | ϕ_{jb}^* | ϕ_{jb}'/r | ϕ_{js}^* | ϕ_{js}'/r |
| 1 | Au-Cu | 1st | 40.4 | 1.5 | 40.4 | 0.8* |
| 2 | Cu-Cu | 1st | 11.1 | -1.0 | 13.3** | -0.3* |
| 3 | Au-Au | 2nd | -5.1 | -4.6 | -5.1 | -4.6 |
| 4 | Cu-Cu | 2nd | 4.1 | 1.1 | 4.1 | 1.1 |

* indicates the modified surface tension terms used in Figure 4a.

**indicates the modified surface force constant term used in Figure 4b.

To characterize the surface modes, a slab calculation¹⁴ was performed with 16 atomic layers, the last of which was attached to a rigid substrate. Due to reflection symmetry through the chosen scattering plane, the sagittal modes [shear vertical (SV) and longitudinal] decouple from the shear horizontal (SH) modes. Selection rules dictate that our experiment was sensitive only to sagittal modes. Calculating these modes required diagonalizing a 64x64 dynamical matrix yielding 64 slab-normalized eigenvectors, of which only a few are strongly localized to the surface region. Helium scattering is most sensitive to SV polarization, so that only modes whose squared SV amplitude in the top layer exceeded 0.5 were considered likely to be observed in our experiment.

When the theoretical surface derived using the bulk force constants is allowed to relax,¹⁵ ("driven" by the nonzero values of ϕ_j'), the Cu atoms shift upwards 0.2 Å out of the surface plane, while the Au positions are unchanged. Hence the surface "rumples". However, experimental studies of the atomic geometry of Cu₃Au(001)¹⁶ and 0.5 ML Au/Cu(001)¹⁷ seem to show that the Au is displaced outward from the Cu by 0.1 Å, differing from the initial theoretical prediction. To compensate for the geometric discrepancy between

this simple model's prediction and the experimentally observed rumpling, the magnitudes of ϕ_{1b}' and ϕ_{2b}' were decreased to produce the experimentally observed structure (see Table 1). A prediction for the surface phonon data using these modified tensions, ϕ_{1s}' and ϕ_{2s}' , is shown in Figure 4a. In this slab calculation the Rayleigh mode agrees well with experiment, but the upper mode is too low in energy.

To fit the higher energy mode, the force constant ϕ_{2b}'' between the first layer Cu atoms and the second layer Cu atoms was stiffened by 20%. (Figure 4b). Stiffening ϕ_{2s}'' only slightly affects the Rayleigh wave, while it greatly influences the optical mode. This can be understood by considering the phonon displacement vectors. At $Q = M'$, the Rayleigh wave displacement vectors involve SV motion of the first layer Au atoms, while the first layer Cu atoms remain essentially stationary. However, for the optical mode, the first and second layer Cu atoms vibrate normal to the surface plane 180° out of phase with each other, while the first layer Au atoms vibrate in plane. Hence, the optical mode at $Q = M'$ is more sensitive to force constant changes involving the first and second layer Cu atoms.

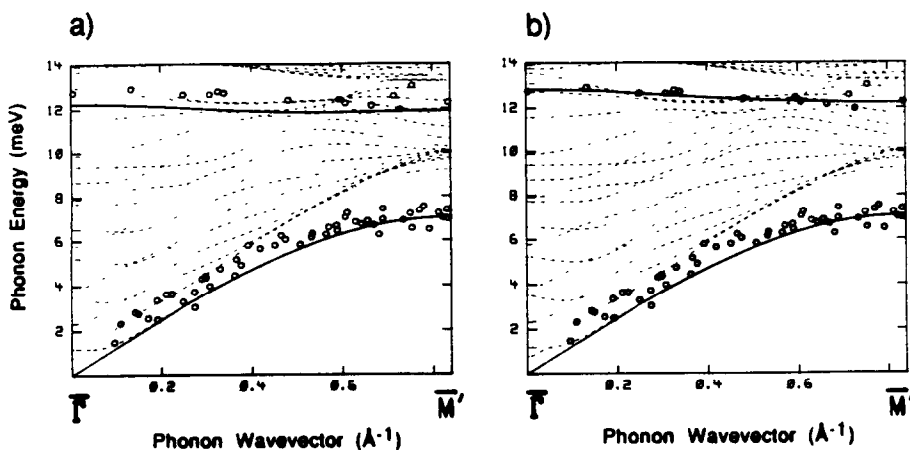


Figure 4: Lattice dynamical calculations for various geometries and force constant changes (see text). a) relaxed positions corresponding to the experimental data^{16,17} and using the bulk force constants.¹³ b) same relaxed positions as in (a) but with a 20% stiffened force constant connecting first and second layer Cu atoms.

The 20% force constant stiffening between the first and second layer Cu atoms resembles the amount of stiffening needed to match the EELS experimental data for the Rayleigh wave on Cu(001).¹⁸ In fact, the force constants in the disordered state of Cu₃Au are almost equal to the force constants in bulk Cu.¹⁹ However, in the ordered phase of bulk Cu₃Au, the bulk Au-Cu first nearest neighbor force constant, ϕ_{1b} , (which is about 3/2 stronger than the Au-Cu bulk force constant of disordered Cu₃Au), is five times the strength of the bulk Cu-Cu force constant, ϕ_{2b} . This suggests that the surface vibrational properties of the Cu₃Au(001) surface in the disordered state may be very similar to the Cu(001) surface.

Of further interest will be the change in the phonon spectrum as the phase transition is approached. Recent neutron scattering work²⁰ indicates that a spinodal transition may occur below T_c , ($T_s = T_c - 24$ K), since the bulk phonon modes near the $\bar{\Gamma}$ point seem to broaden and merge into one peak, starting near $T = 641$ K. Whether similar behavior is seen at the surface will be explored in further experiments.

In conclusion, we have presented phonon dispersion results along the $\langle 100 \rangle$ direction for the ordered Cu₃Au(001) surface, where two surface modes are detected. Using a central potential force constant fitting procedure we have concluded that a 20% stiffening of the force constant between the first and second layer Cu atoms is needed, and that slight relaxations of the first layer nearest neighbor tensions are necessary to match the experimental data. Ab initio calculations would be useful in both the ordered and disordered states to explain the change in bonding as this phase transition occurs.

Acknowledgments

We would like to thank T. M. Buck at Bell Labs for providing the Cu₃Au sample and S. Katano at the Atomic Energy Research Institute in Japan who provided algebraic results which greatly simplify the analysis of bulk phonons a crystal with $L1_2$ symmetry. This work was supported, in part, by the Air Force Office of Scientific Research, the National Science Foundation Materials Research Laboratory at the University of Chicago, and the Research Corporation.

References

1. For a recent review of some of the surfaces that have been studied see; Phonons 89, editors S. Hunklinger, W. Ludwig, and G. Weiss, (World Scientific, Singapore, 1990), p. 841.; or Surf. Sci. **211/212**, (1989).
2. M. Mostoller, R. M. Nicklow, D. M. Zehner, S.-C. Lui, J. M. Mundenar, and E. W. Plummer, Phys Rev. B **40**, 2856 (1989).
3. M. Wuttig, W. Hoffmann, E. Preuß, R. Franchy, H. Ibach, Y. Chen, M. L. Xu, and S. Y. Tong, preprint.
4. A. I. Taub, and R. L. Fleisher, Science **243**, 616 (1989).; B. H. Kear, Scientific American **255**, 159 (1986).; R. L. Fleisher, D. M. Dimiduk, and H. A. Lipsitt, Annu. Rev. Mater. Sci. **19**, 231 (1989).
5. E. G. McRae and R. A. Malic, Surf. Sci. **148**, 551 (1984).
6. R. Lipowsky, Ferroelectrics **73**, 69 (1987); Phys. Rev. Lett. **49**, 1575 (1982).
7. S. F. Alvarado, M. Campagna, A. Fattah, and W. Uelhoff, Z. Phys. B-Condensed Matter **66**, 103 (1987); H. Dosch, and J. Peisl, Colloque de Physique **C7**, 257 (1989).
8. J. F. van der Veen, and J. W. M. Frenken, Surf. Sci. **178**, 382 (1986).
9. B. Gans, Ph. D. thesis, The University of Chicago, 1990.
10. D. D. Koleske, Y. W. Yang, B. I. Gans, S. F. King, W. Menezes, S. Silence, H. Krebs, and S. J. Sibener, (to be published).
11. G. W. Graham, Surf. Sci. **187**, 490 (1987).
12. G. W. Graham, Surf. Sci. **137**, L79 (1984).
13. S. Katano, M. Iizumi and Y. Noda, Phys. F: Met. Phys. **18**, 2195 (1988).
14. R. E. Allen, G. P. Alldredge, and F. W. de Wette, Phys. Rev. **B4**, 1648 (1971).
15. T. E. Feuchtwang, Phys. Rev. **155**, 715 (1967).
16. Z. Q. Wang, Y. S. Li, C. K. C. Lok, J. Quinn, F. Jona, and P. M. Marcus, Solid State Comm. **62**, 181 (1987)
17. J. C. Hansen, M. K. Wagner, and J. G. Tobin, Solid State Comm. **72**, 319 (1989).
18. M. Wuttig, R. Franchy, and H. Ibach, Z. Phys. B-Condensed Matter **65**, 71 (1986).
19. E. D. Hallman, Can. J. Phys. **52**, 2235 (1974).
20. E. C. Svensson, E. D. Hallman, and B. D. Gaulin, Phonons 89, Eds. S. Hunklinger, W. Ludwig, and G. Weiss, (World Scientific, Singapore, 1990), p. 1129.; Phys. Rev. Lett. **64**, 289 (1990).